PCCP

Structure of the (10$\bar{1}$4) surfaces of calcite, dolomite and magnesite under wet and dry conditions

Kate Wright,*†[ac] Randall T. Cygan[b] and Ben Slater[c]

[a] *Department of Earth Sciences, University of Manchester, Oxford Road, Manchester, UK M13 9PL*
[b] *Geochemistry Department, Sandia National Laboratories, Albuquerque, NM 87185-0750, USA*
[c] *Royal Institution, Albemarle Street, London, UK W1S 4BS. E-mail: kate@ri.ac.uk*

Received 28th July 2000, Accepted 15th December 2000
First published as an Advance Article on the web 31st January 2001

Atomistic computer simulation methods have been employed to model the structure of the (10$\bar{1}$4) surfaces of calcite ($CaCO_3$), dolomite [$CaMg(CO_3)_2$] and magnesite ($MgCO_3$). Our calculations show that, under anhydrous vacuum conditions, calcite undergoes the greatest degree of surface relaxation with rotation and distortion of the carbonate group accompanied by movement of the calcium ion. The magnesite surface is the least distorted of the three carbonates, with dolomite being intermediate to the two end members. When water molecules are placed on the surface to produce complete monolayer coverage, the surfaces of all three carbonate minerals are stabilized and the amount of relaxation in the surface layers substantially reduced. Of the three phases, dolomite shows the strongest and highest number of interfacial hydrogen bonds between water and the carbonate mineral surface. These calculations suggest that the equilibrium $H_2O + CO_3^{2-} \rightleftharpoons HCO_3^- + OH^-$ will favour the production of hydrogen carbonate ions most strongly for dolomite, less strongly for calcite, and least likely for magnesite.

Introduction

Knowledge of the structure of mineral surfaces at the atomic level is of fundamental importance when considering processes such as growth, dissolution and sorption of impurities. Over the past two decades improvements in surface science techniques such as surface probe microscopy (SPM), X-ray photoelectron spectroscopy (XPS) and X-ray adsorption fine structure (XAFS) have led to an increase in our understanding of mineral surface behaviour. However, these methods are unable to give detailed structural and dynamic information on the relaxed structure of the surface at the atomic level. By using computer simulation techniques in combination with experiment it is possible to develop more realistic models of mineral surfaces and hence gain a greater insight into those processes of interest.

The surface reactivity of calcite ($CaCO_3$), and of the related carbonate minerals dolomite [$MgCa(CO_3)_2$] and magnesite ($MgCO_3$), is a key factor in the chemical control of aquatic environments, in diagenesis, the cycling and entrapment of metal contaminants, in the biogeochemical cycle of carbon, and in a variety of industrial processes. Calcite is the most commonly occurring of the carbonate minerals and its surfaces, the (10$\bar{1}$4) in particular, have been extensively studied by a range of surface analytical techniques. For example, a combination of XPS and low energy electron diffraction (LEED) has been used to study calcite surfaces under exposure to air and aqueous solutions,[1,2] while relaxations of the surface under hydrous conditions have been observed with atomic force microscopy (AFM).[3] These studies indicate only minimal relaxation of the surface through rotation of the CO_3 group when exposed to aqueous fluids. Fenter *et al.*[4] proposed a model based on high resolution X-ray reflectivity whereby the (10$\bar{1}$4) calcite surface, when covered by a monolayer of H_2O, relaxes by rotation and tilting of the carbonate groups down towards the surface. However, there remains some uncertainty as to the detailed atomic structure of the calcite surface at the mineral–fluid interface. Computational studies[5–7] have provided insights into the structure and relative stability of a range of calcite surfaces under both wet and dry conditions which are in good general agreement with experimental data.

By contrast, very little is known of the surface structure of the related minerals dolomite and magnesite at the atomic level although there is considerable interest in their chemical reactivity. Both are common in the geological past yet form only in small quantities in modern marine environments. Surface complexation models have been developed for dolomite[8,9] and for magnesite[10] in order to understand more fully the mechanisms of dissolution and growth under a range of pH conditions. In addition, computational studies[11] have calculated the relative energetics and stability of dolomite surfaces. The aim of the present study is to investigate the detailed surface structure of the (10$\bar{1}$4) perfect cleavage surfaces of calcite, dolomite and magnesite under both hydrous and anhydrous conditions using atomistic computer simulation methods. We utilize the interatomic potential set of Fisler *et al.*[12] that was developed for the accurate simulation of the structure and properties of the rhombohedral carbonate phases.

Computational methods

Atomistic simulation methods are based on the Born model of solids where interatomic potential functions are defined to model the long- and short-range forces acting between atoms or ions in the solid. Oxygen ion polarizability is described by the shell model[13] while directionality of the bonding is

† Currently at the Royal Institution, to where correspondence should be addressed.

DOI: 10.1039/b006130l

Table 1 Short-range potential parameters for water–carbonate interactions

Pair	A/eV	ρ/Å	C/ev Å^6
O_L–O_W	60 599.94	0.1983	21.8435
O_L–H	396.27	0.230	0.0
Ca–O_W	1249.037	0.2891	0.0
Mg–O_W	506.9882	0.309 26	0.0

described by three-body and four-body terms. Simulations are carried out using standard energy minimization schemes in which the energy of the system is calculated with respect to all atomic coordinates. Thus the equilibrium positions of the ions are evaluated by minimizing the lattice energy until all forces acting on the crystal (or surface) are close to or equal to zero. A more comprehensive review of atomistic simulation methods can be found in Cormack.[14]

For the calculation of surface structures, the most commonly used approach is to treat the crystal as planes of atoms which are periodic in two dimensions. Surfaces are modelled by considering a single block, whereas two blocks together simulate the bulk, or a more complex interface. The simulation block is divided into two regions, a near-surface region, Region 1, comprising those atoms adjacent to the surface or interface, and an outer region, Region 2. The atoms in Region 1 are allowed to relax to their minimum energy configuration, while the ions of Region 2 are held fixed at their bulk equilibrium positions. The specific surface energy is defined as the energy per unit area required to form the crystal surface relative to the bulk. The surface energy (γ) is therefore given by:

$$\gamma = \frac{U_s - U_b}{A} \quad (1)$$

where U_s refers to the energy of Region 1 for the surface, U_b refers to the energy of an equivalent number of bulk atoms and A is the surface area. The lower the surface energy, the more stable the surface will be.

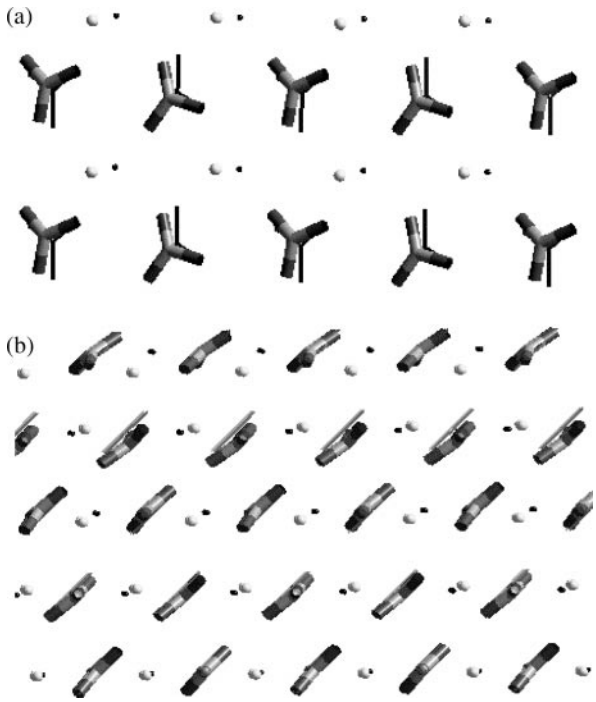

Fig. 1 The structure of the relaxed (10$\bar{1}$4) surface of calcite seen from above (a), and from the side with ($\bar{1}$2$\bar{1}$0) in the plane of the paper (b). The thin black lines and dots represent the bulk unrelaxed positions of the carbonate groups and Ca ions respectively.

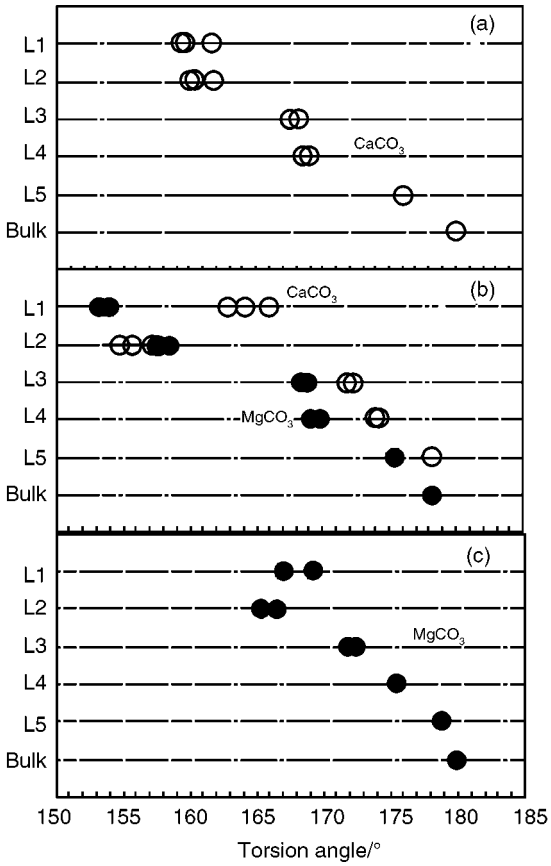

Fig. 2 Calculated torsional angles of the CO_3 groups as a function of layer depth for (a) calcite, (b) dolomite and (c) magnesite, where filled circles represent CO_3 associated with Mg and open circles with Ca.

In the present study, we use the fully transferable potential parameter set of Fisler *et al.*[12] to model carbonate mineral surfaces while water molecules are described by the shell model potential of de Leeuw and Parker.[15] In a recent study of hydrated calcite surfaces, de Leeuw and Parker[5] derive a set of calcite–water interaction parameters which are compatible with those of the water and calcite models used. A new set of parameters to describe carbonate–water interactions has been derived to be consistent with our potentials and is given in Table 1. The initial values of our Buckingham A parameters were taken to have the same ratio as those of the carbonate as was the case in the de Leeuw and Parker[5] model. Values for the ρ and C parameters were kept fixed at the carbonate value. This potential set was then modified by fitting to the structure of ikaite ($CaCO_3 \cdot 6H_2O$). The same scaling factor was also used to modify the Mg–water Buckingham A parameter. All surface calculations were carried out using the MARVIN code[16] with a two-dimensional repeating simulation cell containing 600 ions where the (10$\bar{1}$4) surface was bounded by the ($\bar{1}$014) and ($\bar{1}$2$\bar{1}$0) planes and has an area of 24.25 nm^2 (2 × 1 surface repeat vectors). The Region 1 and 2 sizes (five and seven layers) were obtained by converging the surface and total energies respectively. Associated calculations of bulk properties of the carbonate phases were carried out using the General Utility Lattice Program (GULP).[17]

Results

Anhydrous surfaces

The anhydrous (10$\bar{1}$4) surface was simulated for all three carbonate minerals, which essentially mimics the expected condi-

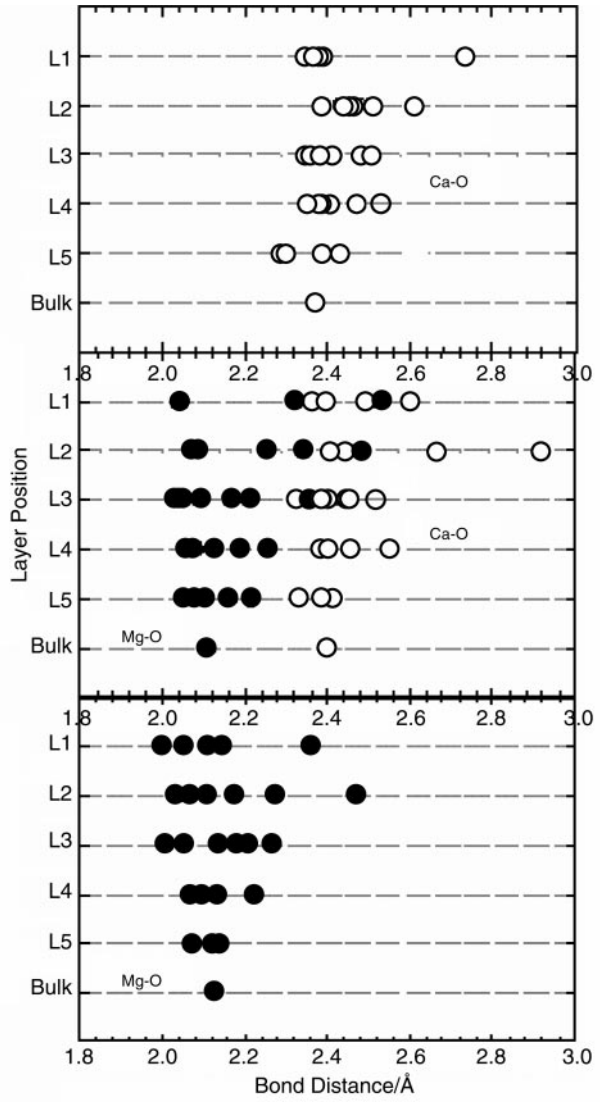

Fig. 3 Ca–O (open circles) and Mg–O (filled circles) octahedral distances as a function of layer depth in (a) calcite, (b) dolomite and (c) magnesite.

tions under a dry vacuum environment. The detailed structure for the calcite surface is shown in Fig. 1 and illustrates the manner in which the surface has reconstructed to accommodate dangling bonds ($Ca\cdots OCO_2$) produced on cleavage. The molecular CO_3 group can be thought of as having three different oxygen types, one above the plane (O1) which in the topmost layer (L1) is underbonded, one in the plane (O2) and one below (O3). The whole group has rotated [Fig. 1(a)] and distorted in a convex manner, with O1 and O2 bending down towards the bulk, while in the second layer the sense of distortion is concave, with O2 and O3 tilting upwards [Fig. 1(b)]. The central C atoms move down by only 0.04 Å in L1. The movements described above are most pronounced for the top two layers which form a convex/concave pair, although a total of five layers were needed in Region 1 before the system converged to the bulk structure. This is illustrated in Fig. 2(a), which gives the calculated torsional angles for the relaxed CO_3 group as a function of depth through the five effective surface layers down to the bulk. The dihedral or torsion angle is measured across the O–C–O–O position and indicates the out-of-plane distortion of the planar group. Additionally, the Ca position moves in the plane of the surface during relaxation. In the top layer (L1), the Ca moves down by -0.75 Å and in plane by -0.71 Å, while in L2, the movement is 0.16 Å up and 0.52 Å in plane, in the opposite sense to the layer above. In the bulk, Ca is octahedrally coordinated to oxygen with a calculated Ca–O distance of 2.37 Å, but in the top layer the octahedron is truncated and in L2 is very distorted giving Ca–O distances ranging from 2.35 to 2.73 Å as shown in Fig. 3(a). In our calculations, which have been confirmed by molecular dynamics simulations, the surface of calcite retains its (1×1) symmetry for these various reconstructions.

The surfaces of dolomite and magnesite also show some distortion of the carbonate group, but to a lesser extent than that exhibited in calcite. Variation in torsion angles for the CO_3 groups and in cation–O octahedral distances are shown in Figs. 2 and 3 respectively, while the structure of the three surfaces can be compared in Fig. 4. As in calcite, movement occurs in the opposite sense for alternate layers. Of the three carbonates considered, magnesite is the most rigid and exhibits the least distortion on relaxation with Mg moving only 0.36 Å in L1 and 0.43 Å in L2 from the bulk positions, compared to 1.05 Å and 0.55 Å in L1 and L2 respectively for Ca in calcite. This type of behaviour reflects differences in the bulk moduli of the three carbonates, where magnesite is the least compressible and calcite the most.[12] Similarly, the CO_3 groups exhibit less rotation and less deviation in dihedral angles in magnesite (Fig. 2). Dolomite appears to exhibit a mixed behaviour with respect to these distortions part way between the two single cation end members. The movement of Ca and Mg away from their initial bulk positions in L1 is 0.70 Å and 0.97 Å respectively. Distortions of the carbonate groups

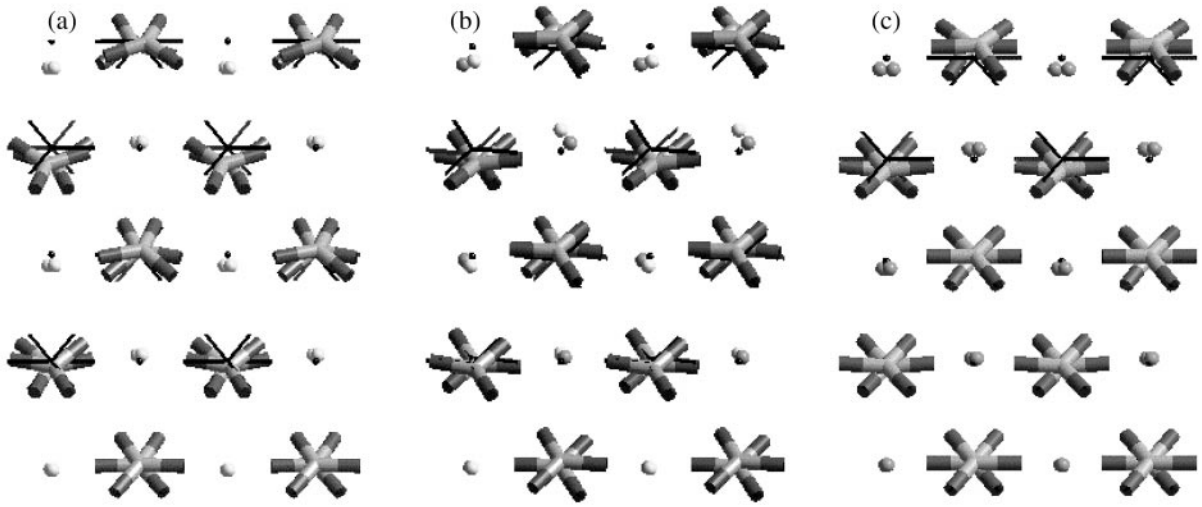

Fig. 4 Comparison of the structure of calcite, dolomite and magnesite relaxed $(10\bar{1}4)$ surfaces viewed from the side with $(\bar{1}014)$ in the plane of the paper. Black lines and dots show the bulk unrelaxed structure as in Fig. 1.

are also different depending on whether the group is associated with a Ca or Mg ion [Fig. 2(b)] and results in the canting of alternate CO_3 groups giving a crenellated surface structure.

Wet surfaces

The surfaces of calcite, dolomite and magnesite were hydrated with a complete monolayer of water, *i.e.* one water molecule per surface cation. The molecules were initially placed with the plane of the water molecule lying parallel to the surface in such a way as to produce a herringbone motif when viewed from above. The water O atoms were placed at a distance of 2.4 Å above the surface Ca or Mg, the optimum height for calcite found by de Leeuw and Parker.[5] The surface and water molecules were then allowed to relax to their minimum energy structure. A systematic exploration of initial monolayer configurations was carried out with the arrangement described above giving the lowest energy. The variation in CO_3 group torsional angles for the relaxed calcite surface with a monolayer of water is shown in Fig. 5. In calcite, the hydrated surface shows very little difference from the bulk below L3, and the degree of relaxation in L1 and L2 is substantially reduced compared to the dry surface. Ca moves from its bulk position by only 0.26 Å in L1 when water is present compared to 1.05 Å for the dry surface. The water molecules lie almost flat on the surface (hydrogens angled slightly upwards) and have an average Ca–O_W distance of 2.55 Å [Fig. 6(a)]. This value is in excellent agreement with the experimental X-ray reflectivity data for the calcite–water system.[4] A similar geometry was found for the water layer on magnesite [Fig. 6(c)] where the average Mg–O_W distance is longer at 2.76 Å. Dolomite exhibits mixed behaviour, with Ca–O_W and Mg–O_W distances of 2.45 Å and 3.02 Å respectively, where the hydrogens of water molecules above Ca are again angled slightly upwards, but those over the Mg lie flat as shown in Fig. 6(b). Measurement of $CO_3\cdots H$ distances indicates that the water lying above the Mg forms two strong hydrogen bonds per molecule at 2.02 Å, whilst water above the calcium site forms three weaker hydrogen bonds of 2.24–2.36 Å per molecule. This contrasts with calcite, where one hydrogen bond per H_2O is formed at 2.36 Å, and with magnesite which displays nearest neighbour $CO_3^{2-}\cdots H^+$–OH^- distances of 2.56 Å.

The hydration energies are calculated by comparing the energy of the surface with *n* adsorbed water molecules, to a bare surface plus *n* water molecules in the gas phase. Since we wish to consider liquid water on the surface, when calculating hydrated surface energies, we must add the energy for $H_2O(l)$ rather than $H_2O(g)$. We use the values of de Leeuw and Parker[15] which were calculated using a molecular dynamics approach and the identical potential parameters for water as used in this study. The energy difference between liquid and gas is then the condensation energy, which is given as −43.0 kJ mol^{-1} and compares extremely well with the experimental value of −43.4 kJ mol^{-1}. The surface energy for the hydrated surface is obtained by:

$$\gamma_{wet} = \frac{U_{s,\,wet} - (U_b + U_w)}{A} \qquad (2)$$

where $U_{s,\,wet}$ represents the potential energy of the relaxed hydrated surface and U_w the potential energy of the *n* water molecules [$H_2O(l)$]. Calculated hydration energies per water molecule and wet surface energies are presented in Table 2 and further illustrate the way in which water stabilizes these surfaces by significantly reducing the degree of relaxation experienced and hence the lowering of the surface energy. Our

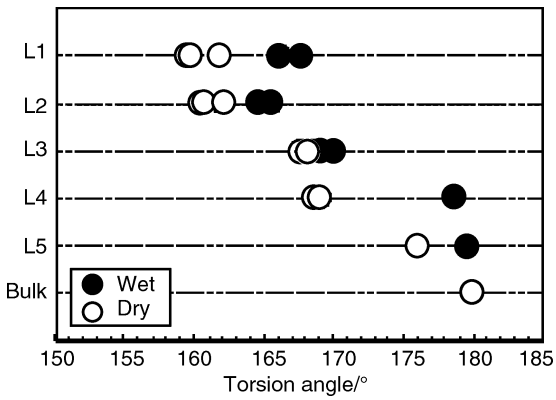

Fig. 5 Comparison of torsional angles for the wet and dry surface of calcite.

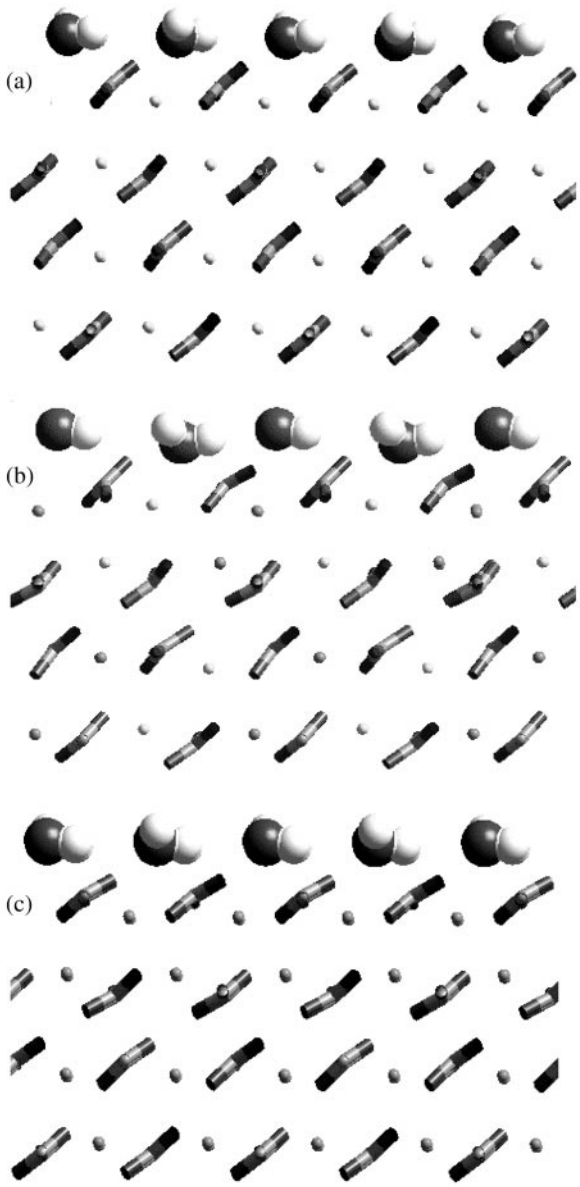

Fig. 6 Structure of the hydrated surfaces of (a) calcite, (b) dolomite and (c) magnesite showing the structure of the adsorbed monolayer of water.

Table 2 Hydration energies (per molecule) for monolayer coverage on carbonate surfaces, and wet and dry surface energies

	E_{hyd}/kJ mol^{-1}	γ_{dry}/J m^{-2}	γ_{wet}/J m^{-2}
Calcite	−53.9	0.322	0.232
Dolomite	−52.1	0.247	0.165
Magnesite	−60.7	0.256	0.084

calculations show that the dry calcite surface is the least stable, and therefore the most reactive and dolomite the most stable. However, when hydrated, magnesite is stabilized relative to dolomite and calcite although calcite is still predicted to be the most reactive of the three carbonates.

Discussion

Our calculations show that the anhydrous $(10\bar{1}4)$ surfaces of calcite, dolomite and magnesite are all stabilized when covered by a monolayer of water. This can be rationalized by considering the coordination of the surface cations. In the bulk carbonate structures, each metal cation is octahedrally coordinated by six oxygens, each from a different CO_3 group. Formation of the $(10\bar{1}4)$ surface leads to a configuration with only a five-coordinated metal cation present at the surface and therefore the surface must restructure to compensate. This under-coordination causes the cation to displace into the surface towards the bulk and the CO_3 groups to distort and tilt as shown in Fig. 1(b) for calcite. The magnitude of these atomic movements in the top surface layer is such that subsequent layers also need to reorganize, down to a depth of at least four layers. When water is added to the surface, the cation is then able to coordinate to the water oxygen thus forming a stable octahedral ion shell. This more favourable configuration stabilizes the surface and significantly reduces the surface energy and degree of relaxation in the top layer, which in turn means that the layers beneath experience less stress and hence less need to reorganize. For the hydrated surfaces, the bulk configuration is reached at three layers below the surface rather than the five layers required under dry conditions.

There are some differences in how the water molecules are configured on the relaxed $(10\bar{1}4)$ surface for each of the three carbonate phases. As indicated in Fig. 6(a), the water molecules for the saturated monolayer configuration on calcite are arranged above each calcium ion and are slightly angled above the surface plane with the hydrogen atoms pointing away from the surface. The mean $Ca–O_W$ distance of 2.55 Å is slightly greater than the bulk Ca–O distance of 2.37 Å. A similar structure is found for the hydrated magnesite surface [Fig. 6(c)] but with a mean $Mg–O_W$ distance of 2.76 Å, substantially greater than the bulk magnesite $Mg–O_L$ distance of 2.13 Å. This behaviour can be explained by considering the effective charge of the O_W as compared to that of O_L which is much larger and hence experiences a greater attraction to the Mg cation.

The hydration of the $(10\bar{1}4)$ surface of dolomite involves the coordination of water molecules to both calcium and magnesium surface ions. Inspection of Fig. 6(b) reveals distinctive features in the surface and water layer structure. This mixed cation phase shows alternate cation displacement into the structure in the first and third layers, whilst in the second and fourth layers the ions lie in the same plane (see also Fig. 2). This can be rationalized in terms of the relative ionic radii of Ca^{2+} and Mg^{2+}, since the Mg^{2+} ion is smaller and thus has a shorter $Mg–CO_3^{2-}$ distance than Ca^{2+}; therefore the first coordination shell of Mg is smaller than Ca. This leads to significant out-of-plane distortion of the carbonate groups, manifesting itself as alternate canting of the surfacial carbonate groups coupled with displacement of the Mg ion into the surface. This effect in turn leads to canting of the monolayer water molecules such that half of the adsorbed water molecules (those proximate to the Mg sites) are oriented with their dipole pointing away from the surface. This is in contrast to those water molecules oriented into this surface at the Ca sites and in the two end member phases.

Since the Mg ion is less accessible in the first surface layer, the water is less strongly bound such that the $Mg\cdots OH_2$ distance lengthens to 3.05 Å from the 2.76 Å found in magnesite. It is also interesting to note that the strongest hydrogen bonds occur with dolomite rather than calcite or magnesite. Clearly our potential model does not permit hydrolysis, and although our surface has only monolayer coverage, these calculations suggest that the $CO_3^{2-} + H_2O \rightleftharpoons HCO_3^- + OH^-$ equilibrium would favour $CO_3^{2-}\cdots H^+$ formation at the dolomite–water interface more strongly than for the other two phases considered here. Thus, we predict that the hydrated dolomite surface will show the shortest (and therefore the most strongly coordinated) $CO_3^{2-}\cdots H^+$ distances at the interfacial region. These water–surface distances calculated for dolomite, along with those of calcite and magnesite, are likely to be longer in the real system, where more than one layer of water will be present. Additional water layers will screen hydrogen bond interactions between water and CO_3^{2-} and therefore we expect that our values represent the lower limit of water–surface distances.

Our results for the dry $(10\bar{1}4)$ surface of calcite are consistent with the XPS and LEED data[1,2] which have been interpreted in terms of a restructuring at the surface by the rotation and downward relaxation of the CO_3 groups. There have been a number of studies which have looked at the structure of the $(10\bar{1}4)$ surface of calcite in contact with aqueous fluids. Data from X-ray reflectivity experiments[4] are consistent with a model of the surface–water interface in which the top two layers of the surface are relaxed. In this model, the adsorbed monolayer of H_2O has a height of 2.50 ± 0.12 Å relative to the surface Ca positions which is in excellent agreement with our predicted height of 2.55 Å relative to the same position. AFM images of the wet calcite surface[3] show different heights for the surface CO_3 groups leading to a loss of the (1×1) symmetry, although we find no evidence to support this in our calculations. Calculations by de Leeuw and Parker[5] found that the AFM data[3] could be reproduced for partial water coverage but not for the full monolayer coverage.

The simulations of de Leeuw and Parker[5] provide a similar geometry of the hydrated calcite surface to those presented here using the carbonate potential of Pavese *et al.*[18] and a polarizable water model potential.[19] Their calculated energies for dry and wet $(10\bar{1}4)$ surface of calcite are 0.6 J m^{-2} and 0.3 J m^{-2} respectively compared to our values of 0.32 J m^{-2} and 0.23 J m^{-2}. There are a number of differences between the parameter sets used by de Leeuw and Parker[5] and those used in this study. Firstly, the carbonate potential of Fisler *et al.*[12] contains different inter- and intramolecular O–O interaction parameters to act between and within the CO_3^{2-} molecular anions. In the Pavese *et al.*[18] model the same parameter is used for both. Secondly, the earlier water model has a different charge distribution between the oxygen core and shell. Because the surface energies are acutely sensitive to the potential parameters used, it is not surprising that our reported energies are different. However, trends shown by the energies should be the same if both parameter sets are valid and indeed we find that this is the case.

Comparison of our results for magnesite and dolomite with experiment is much more problematic, since the surface structure of these minerals has not been so extensively studied. Pokrovsky *et al.*[9,10] have investigated the surface speciation and reactivity of both dolomite and magnesite under hydrous conditions and consider $M\cdots OH_2$ speciation (where M is Ca or Mg) to be important for both systems at moderate pH values. However, no structural models have been proposed for these hydrated surfaces. The computational study by Titiloye *et al.*[11] compared calcite and dolomite surfaces and found that the anhydrous dolomite $(10\bar{1}4)$ surface had a higher surface energy than that for calcite, the opposite of the results presented here. However, their Mg–O potential was different to that used here. The energies associated with our surface simulations are based on a set of interaction potentials that have

successfully modelled the bulk behaviour of carbonate phases and water systems. These potentials used here were derived to be fully transferable between different carbonate minerals[12] and the Region 1 size was fully converged; thus we feel confident that our results are consistent within the limitations of the models employed.

Hydration and surface energies are sensitive to the values obtained for the isolated water molecule and liquid water assemblage, respectively. For this reason, no experimental values for the water energies are incorporated into the energy calculations; only values obtained directly from simulations based on the potentials of de Leeuw and Parker[15] are used. Although surface energies derived from potential-based empirical models are acutely sensitive to the total energies computed, the fact that we have used a fully transferable and coherent set of potentials leads us to believe that the observed trends in the reported energies correctly model the relative behaviour of the mineral surface structures.

Conclusions

We have successfully modelled the $(10\bar{1}4)$ surface structure of the three carbonate phases, calcite, dolomite and magnesite. The calculated surface geometries and energies show that, for the anhydrous surfaces, calcite is the most reactive and undergoes the largest relaxation, while magnesite is the least reactive and is closest to the bulk geometry. When these surfaces are covered by a monolayer of water, all are stabilized relative to the anhydrous surfaces. Water forms $M\cdots OH_2$ complexes on all three surfaces studied. Dolomite shows the shortest $CO_3^{2-}\cdots H^+$ distances, calcite shows intermediate distances whilst magnesite exhibits the weakest bound water complexes.

Acknowledgements

The authors would like to thank P. V. Brady for his comments on the manuscript. KW would like to thank the Royal Society for support under their University Research Fellowship scheme. RTC is grateful for the funding provided by the US Department of Energy, Office of Basic Energy Sciences, Geosciences Research, under contract DE-AC04-94AL85000 with Sandia National Laboratories.

References

1 S. L. Stipp and M. F. Hochella, Jr., *Geochim. Cosmochim. Acta*, 1991, **55**, 1723.
2 S. L. Stipp, *Geochim. Cosmochim. Acta*, 1999, **63**, 3121.
3 Y. Liang, A. S. Lea, D. R. Baer and M. H. Engelhard, *Surf. Sci.*, 1996, **351**, 172.
4 P. Fenter, P. Geissbühler, E. DiMasi, G. Srajer, L. B. Sorensen and N.C. Sturchio, *Geochim. Cosmochim. Acta*, 2000, **64**, 1221.
5 N. H. de Leeuw and S. C Parker, *J. Chem. Soc., Faraday Trans.*, 1997, **93**, 467.
6 N. H. de Leeuw and S. C Parker, *J. Phys. Chem. B*, 1998, **102**, 2914.
7 N. H. de Leeuw, S. C. Parker and J. H. Harding, *Phys. Rev. B*, 1999, **60**, 13792.
8 P. V. Brady, J. L. Krumhansl and H. W. Papenguth, *Geochim. Cosmochim. Acta*, 1996, **60**, 727.
9 O. S. Pokrovsky, J. Schott and F. Thomas, *Geochim. Cosmochim. Acta*, 1999, **63**, 3133.
10 O. S. Pokrovsky, J. Schott and F. Thomas, *Geochim. Cosmochim. Acta*, 1999, **63**, 863.
11 J. O. Titiloye, N. H. de Leeuw and S. C. Parker, *Geochim. Cosmochim. Acta*, 1998, **62**, 2637.
12 D. K. Fisler, J. D. Gale and R. T. Cygan, *Am. Mineral.*, 2000, **85**, 217.
13 B. G. Dick and A. W. Overhauser, *Phys. Rev.*, 1958, **112**, 90.
14 A. Cormack, in *Microscopic Properties and Processes in Minerals* 1999, ed. K. Wright and C. R. A. Catlow, NATO Science Series C 543, p. 337.
15 N. H. de Leeuw and S. C. Parker, *Phys. Rev. B*, 1998, **58**, 13901.
16 D. H. Gay and A. L. Rohl, *J. Chem. Soc., Faraday Trans.*, 1995, **91**, 925.
17 J. D. Gale, *J. Chem. Soc., Faraday Trans.*, 1997, **93**, 629.
18 A. Pavese, M. Catti, G. D. Price and R. A. Jackson, *Phys. Chem. Mineral.*, 1992, **19**, 80.
19 N. H. de Leeuw, G. W. Watson and S. C. Parker, *J. Chem. Soc., Faraday Trans.*, 1996, **92**, 2081.